AMERICAN SOCIETY FOR MICROBIOLOGY | Applied and Environmental Microbiology®

MICROBIAL ECOLOGY

Individual Physiological Adaptations Enable Selected Bacterial Taxa To Prevail during Long-Term Incubations

D. P. R. Herlemann,[a,b] S. Markert,[c,d] C. Meeske,[a] A. F. Andersson,[e] I. de Bruijn,[e] C. Hentschker,[f] F. Unfried,[c,d] D. Becher,[f] K. Jürgens,[a] T. Schweder[c,d]

[a]Leibniz Institute for Baltic Sea Research Warnemünde, Rostock, Germany
[b]Center of Limnology, Estonian University of Life Sciences, Elva Parish, Tartu County, Estonia
[c]Department of Pharmaceutical Biotechnology, Institute of Pharmacy, University of Greifswald, Greifswald, Germany
[d]Institute of Marine Biotechnology e.V., Greifswald, Germany
[e]Science for Life Laboratory, School of Engineering Sciences in Chemistry, Biotechnology and Health, Department of Gene Technology, KTH Royal Institute of Technology, Stockholm, Sweden
[f]Institute of Microbiology, Department of Microbial Proteomics, University of Greifswald, Greifswald, Germany

ABSTRACT Enclosure experiments are frequently used to investigate the impact of changing environmental conditions on microbial assemblages. Yet, how the incubation itself challenges complex bacterial communities is thus far unknown. In this study, metaproteomic profiling, 16S rRNA gene analyses, and cell counts were combined to evaluate bacterial communities derived from marine, mesohaline, and oligohaline conditions after long-term batch incubations. Early in the experiment, the three bacterial communities were highly diverse and differed significantly in their compositions. Manipulation of the enclosures with terrigenous dissolved organic carbon resulted in notable differences compared to the control enclosures at this early phase of the experiment. However, after 55 days, bacterial communities in the manipulated and the control enclosures under marine and mesohaline conditions were all dominated by gammaproteobacterium *Spongiibacter*. In the oligohaline enclosures, actinobacterial cluster I of the hgc group (hgc-I) remained abundant in the late phase of the incubation. Metaproteome analyses suggested that the ability to use outer membrane-based internal energy stores, in addition to the previously described grazing resistance, may enable the gammaproteobacterium *Spongiibacter* to prevail in long-time incubations. Under oligohaline conditions, the utilization of external recalcitrant carbon appeared to be more important (hgc-I). Enclosure experiments with complex natural microbial communities are important tools to investigate the effects of manipulations. However, species-specific properties, such as individual carbon storage strategies, can cause manipulation-independent effects and need to be considered when interpreting results from enclosures.

IMPORTANCE In microbial ecology, enclosure studies are often used to investigate the effect of single environmental factors on complex bacterial communities. However, in addition to the manipulation, unintended effects ("bottle effect") may occur due to the enclosure itself. In this study, we analyzed the bacterial communities that originated from three different salinities of the Baltic Sea, comparing their compositions and physiological activities both at the early stage and after 55 days of incubation. Our results suggested that internal carbon storage strategies impact the success of certain bacterial species, independent of the experimental manipulation. Thus, while enclosure experiments remain valid tools in environmental research, microbial community composition shifts must be critically followed. This investigation of the metaproteome during long-term batch enclosures expanded our current understanding of the so-called "bottle effect," which is well known to occur during enclosure experiments.

Citation Herlemann DPR, Markert S, Meeske C, Andersson AF, de Bruijn I, Hentschker C, Unfried F, Becher D, Jürgens K, Schweder T. 2019. Individual physiological adaptations enable selected bacterial taxa to prevail during long-term incubations. Appl Environ Microbiol 85:e00825-19. https://doi.org/10.1128/AEM.00825-19.

Editor Shuang-Jiang Liu, Chinese Academy of Sciences

Copyright © 2019 American Society for Microbiology. All Rights Reserved.

Address correspondence to D. P. R. Herlemann, Daniel.Herlemann@emu.ee.

D.P.R.H. and S.M. contributed equally to this work.

Received 10 April 2019
Accepted 24 May 2019
Accepted manuscript posted online 31 May 2019
Published 18 July 2019

KEYWORDS Baltic Sea, bottle effect, *Spongiibacter*, enclosure, salinity

In microbial ecology, enclosure experiments are a potent tool that is routinely applied to understand complex interactions and the responses to changes in a variety of ecosystems. Typically, in these types of experiments, the effects of altering one or multiple parameters on microbial assemblages and bulk process rates are assessed and the results then used to predict the potential responses of the microbial community to comparable changes *in situ* (for a review, see reference 1). However, enclosure experiments can introduce biases leading to, e.g., an overestimation of microbial process rates compared to those occurring *in situ* and to significant changes in microbial composition (2–6). Isolation of the assemblage may prevent the exchange of nutrients, organic matter, and organisms that normally occurs in the natural environment. Enclosure experiments with natural microbial communities are usually marked by three distinct phases (7). In the early phase, microbial viability and cultivability increase. The middle phase is characterized by growth of bacterivorous protists and a drop in bacterial cell numbers, whereas in the late phase, bacterial cell numbers increase again but the bacterial community composition differs from the initial one as it includes cells that are less active and probably less sensitive to grazing (5, 8). This typical three-phase succession has been generally associated with the so-called "bottle effect," defined as the nonspecific effect resulting from the confinement itself rather than from the intended manipulation (9); however, the underlying mechanisms remain unclear (9, 10). Studies that investigated the impact of the surface-to-volume ratio of the incubation container on changes in bacterial community composition found no evidence of a volumetric bottle effect for volumes >1 ml (10, 11). Wall growth, i.e., biofilm formation on the walls of the experimental enclosure, was also excluded, as the bottle effect persisted even when the bacterial community was frequently transferred to new bottles (12). In a chemostat experiment, Massana and Jürgens (5) strongly reduced grazing pressure and nutrient limitation by using <2-μm-filtered seawater devoid of larger grazers. This experimental setup avoided the drop in cell numbers that characterizes the middle phase of enclosure experiments and delayed the shift in the microbial community composition for >15 days. Therefore, bacterial grazing is an important factor that influences the enclosure-related shift in bacterial community composition in a system where carbon and nutrients are recycled (5).

In a previous study, bacterial communities from marine, mesohaline, and oligohaline conditions were incubated in batch enclosures manipulated with terrigenous dissolved organic matter (tDOM) (13). The potential of the bacterial communities for tDOM utilization was investigated by correlating high-resolution DOM patterns with changes in the bacterial community composition during the early and middle phases of the *in vitro* cultivations. A grazing event was observed in the middle phase of the enclosure experiment, and after 55 days, the bacterial communities were dominated by only a few bacterial species. Thus, in this subsequent study, we analyzed metaproteomic profiles, 16S rRNA gene-based bacterial community compositions, and cell numbers from the same experiment as described in Herlemann et al. (13), but with a focus on the physiological strategies of the dominant bacteria in the late phase of the experiment. We hypothesized that bacteria that become dominant in long-term enclosure experiments possess, in addition to grazing resistance, physiological peculiarities that support their long-term survival.

RESULTS

Cell numbers and bacterial community composition dynamics. During the incubations, cell numbers in the enclosures were consistent with those previously described for the three phases typical of confinement experiments (Fig. 1) (7). Thus, in the early phase (P1) of the incubations, the numbers of bacterial cells increased under all salinity conditions. This was mainly reflected by an increase in high-nucleic acid (HNA) cells in the marine and mesohaline enclosures. In the oligohaline enclosures,

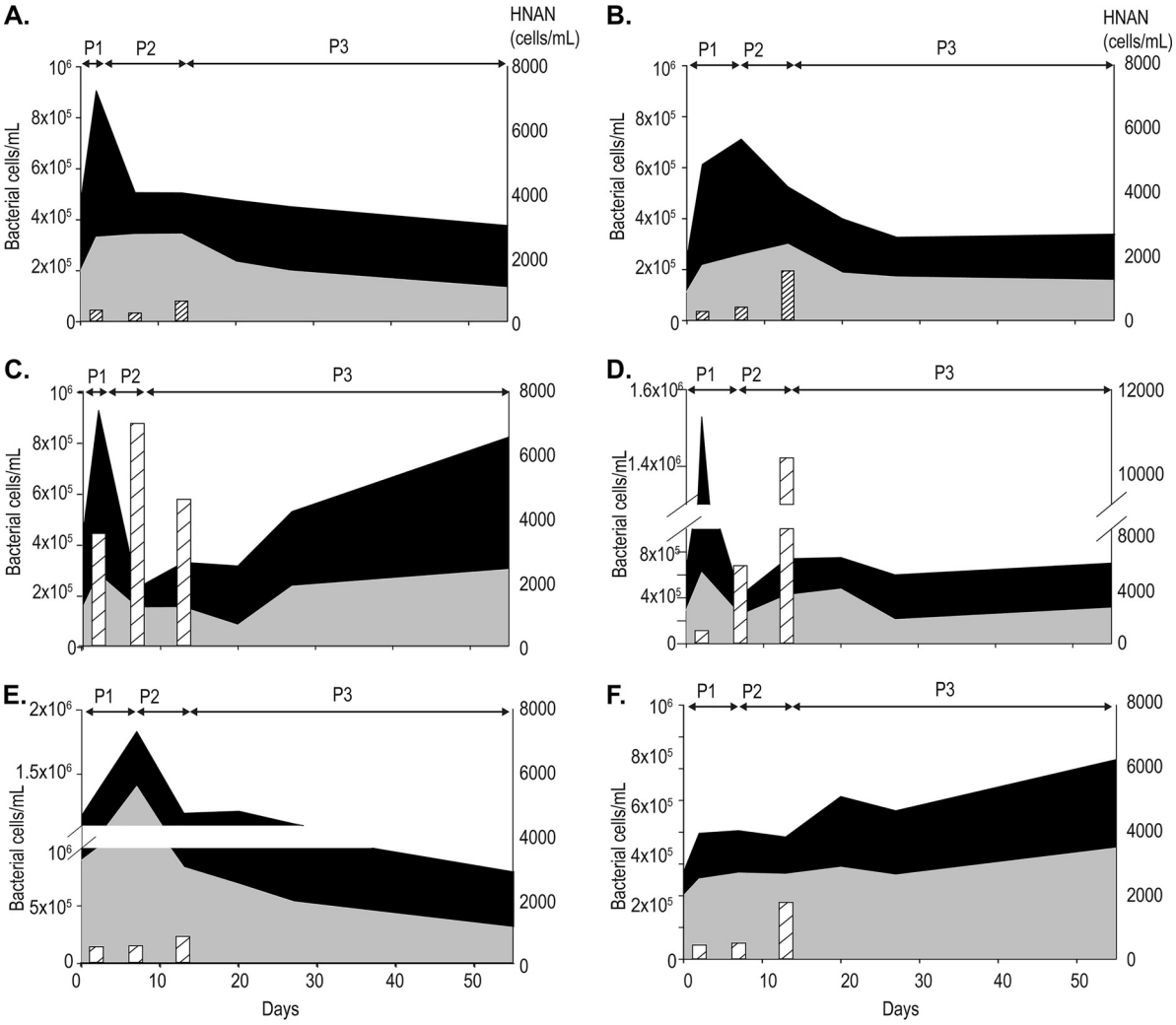

FIG 1 Average cell counts (areas) and heterotrophic and autotrophic nanoflagellate (HNAN) counts of the control (A, C, and E) and terrigenous dissolved organic matter (tDOM) manipulation (B, D, and F) in the marine (salinity 32) (A, B), mesohaline (salinity 7) (C, D), and oligohaline (salinity 3) (E, F) enclosures. The sum of the high-nucleic acid (HNA; black) and low-nucleic acid (LNA; gray) cells is the total number of cells. HNAN counts for days 2, 7, and 12 are shown as bar graphs. The incubation phases (P1 to P3) are indicated at the top of each graph. Shown are the averages from $n = 3$.

HNA and low-nucleic acid (LNA) cell abundances increased at similar rates. In the middle phase (P2), between 3 and 14 days, bacterial cell numbers, especially for HNA cells, dropped dramatically in the marine and mesohaline enclosures, whereas heterotrophic and autotrophic nanoflagellates ($<10\ \mu$m) (HNAN) became abundant. In the oligohaline enclosures (M3), both HNA and LNA cell numbers decreased. Total cell numbers increased again in the late phase (55 days; P3) in all enclosures, with roughly equal proportions of HNA and LNA cells.

Nonmetric multidimensional scaling (NMDS) of the P1 to P3 bacterial community compositions based on 16S rRNA gene analysis (Fig. 2) indicated considerable differences in the bacterial communities of the marine (M1), mesohaline (M2), and oligohaline (M3) enclosures (Fig. 2, vector salinity, coordinate 1, circles, squares, and triangles, respectively). The community structure changed over time during the incubations (Fig. 2, vector time, coordinate 2). Especially prominent differences were noted when comparing the 55-day samples with the initial samples and the 7-day samples (Fig. 2, green symbols versus red and blue symbols, respectively). In contrast to salinity and time, an impact of the tDOM manipulation on bacterial community composition was apparent only in the marine enclosures (Fig. 2, filled versus empty symbols), whereas the effect of added tDOM on the mesohaline and oligohaline enclosures was weak.

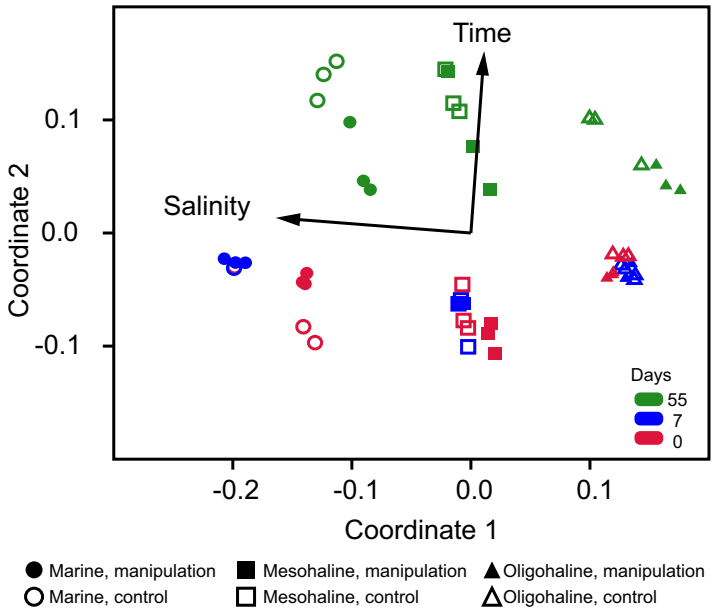

FIG 2 Nonmetric multidimensional scaling (NMDS) plot (Bray-Curtis dissimilarity, stress 0.176) of the 16S rRNA gene-based changes in bacterial community composition (each setup has three parallels). The vectors indicate differences in salinity and the changes over time, and these parameters were added *post hoc* to the NMDS graph.

A detailed analysis of the abundant (>1% per sample) operational taxonomic units (OTUs) based on the 16S rRNA gene analysis indicated that the bacterial communities in the marine enclosures during P1 and P2 consisted of a diverse mixture of *Alphaproteobacteria*, *Betaproteobacteria*, and *Gammaproteobacteria*, including the abundant SAR11, *Roseobacter*, OM43, and SAR86 (Fig. 3, start, 7 days). *Bacteroidetes* and *Actinobacteria* were more abundant, and *Proteobacteria*, especially *Alphaproteobacteria*, were less abundant in the mesohaline and oligohaline enclosures than in the marine

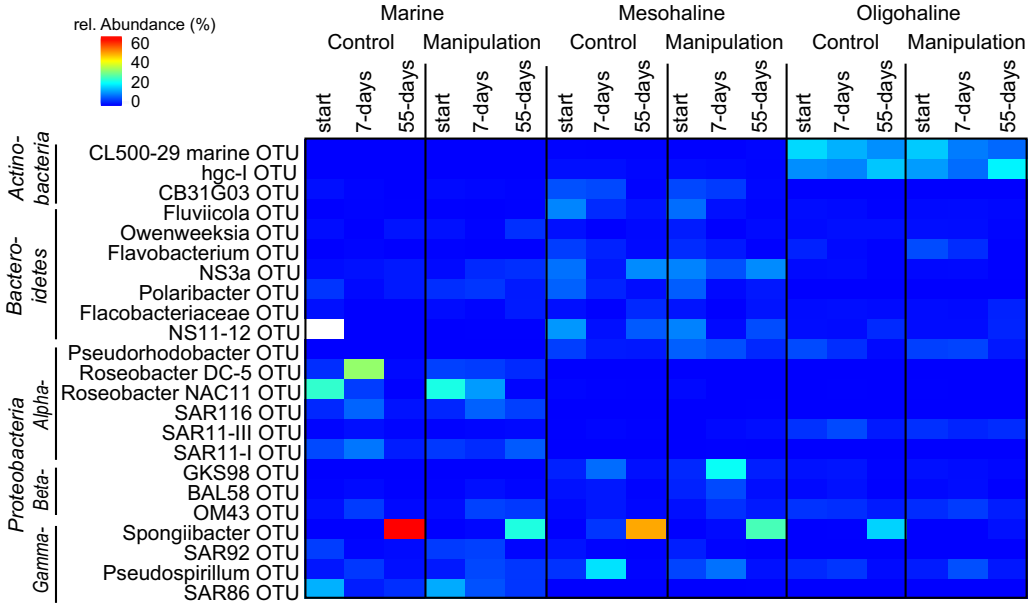

FIG 3 Changes in relative abundances of bacterial taxa (operational taxonomic units [OTUs]) in the enclosure experiments based on the 16S rRNA gene (only OTUs whose relative abundance in the sequences within a sample was >1% are included). Shown are the averages from $n = 3$.

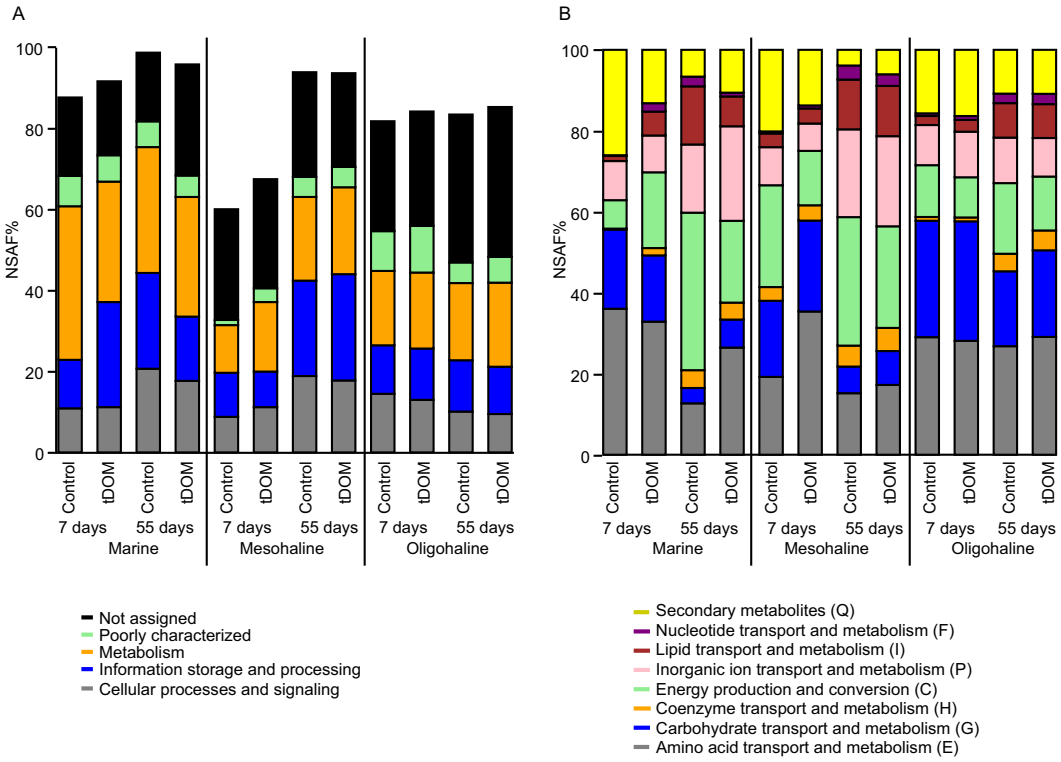

FIG 4 Relative abundance of Clusters of Orthologous Groups (COGs) categories in all samples. (A) Total protein abundances, expressed as normalized spectral abundance factors (NSAF%), of all proteins assigned to the respective general COGs category. Missing from the 100% total are proteins of nonbacterial origin. (B) Distribution of functional COGs categories of bacterial proteins within the general category "metabolism" (set to 100%). Protein abundance values were obtained from the combined database search of two independent biological replicates ($n = 2$) per sample (see Materials and Methods for details).

enclosures. In the mesohaline enclosures, several betaproteobacterial OTUs, including GKS98 and *Pseudospirillum* but also NS3 and *Polaribacter* from the *Bacteroidetes* group, were abundant, whereas *Actinobacteria*, especially CL500-29 and cluster I of the hgc group (hgc-I), dominated the bacterial community of the oligohaline enclosures. In the late phase (P3) of the experiment, the drastic shift in the bacterial community composition was reflected by the dominance of few OTUs (Fig. 3). Thus, the 55-day samples from the marine and mesohaline enclosures contained high abundances (up to 60%) of *Gammaproteobacteria*, specifically, of the genus *Spongiibacter* (previously called *Melitea* or *Zhongshania* [14]), while *Alphaproteobacteria* and *Betaproteobacteria* were less abundant. The *Spongiibacter* OTU was also present in the 55-day samples from the oligohaline condition, albeit in lower abundances. Instead, the late-phase bacterial community in the oligohaline enclosures was still dominated by actinobacterial CL500 and hgc-I OTUs.

Protein expression patterns in the middle and late phases of the experiment. To compare the physiological characteristics of the middle (P2) and late (P3) bacterial communities, metaproteomic profiles of the samples were analyzed (day 7 and day 55, respectively). Totals of 5,703 proteins from the marine enclosures (M1), 9,538 proteins from the mesohaline enclosures (M2), and 8,293 proteins from the oligohaline enclosures (M3) were identified (see Table S1 in the supplemental material). Most of the total identified protein abundance in all samples was accounted for by bacterial (60% to 99%) rather than eukaryotic (0.3% to 33%) proteins (Fig. 4A; see also Fig. S1). Prokaryotic protein identifications belonged to a total of 912 bacterial genera from 53 different classes (see Table S2). The bacterial proteins identified in this study belonged to 1,223 protein families in 21 functional categories (according to the Clusters of Orthologous Groups [COGs] categorization, see Materials and Methods for details) (see Table S3). The changes in bacterial community composition that occurred between P2 and P3 were

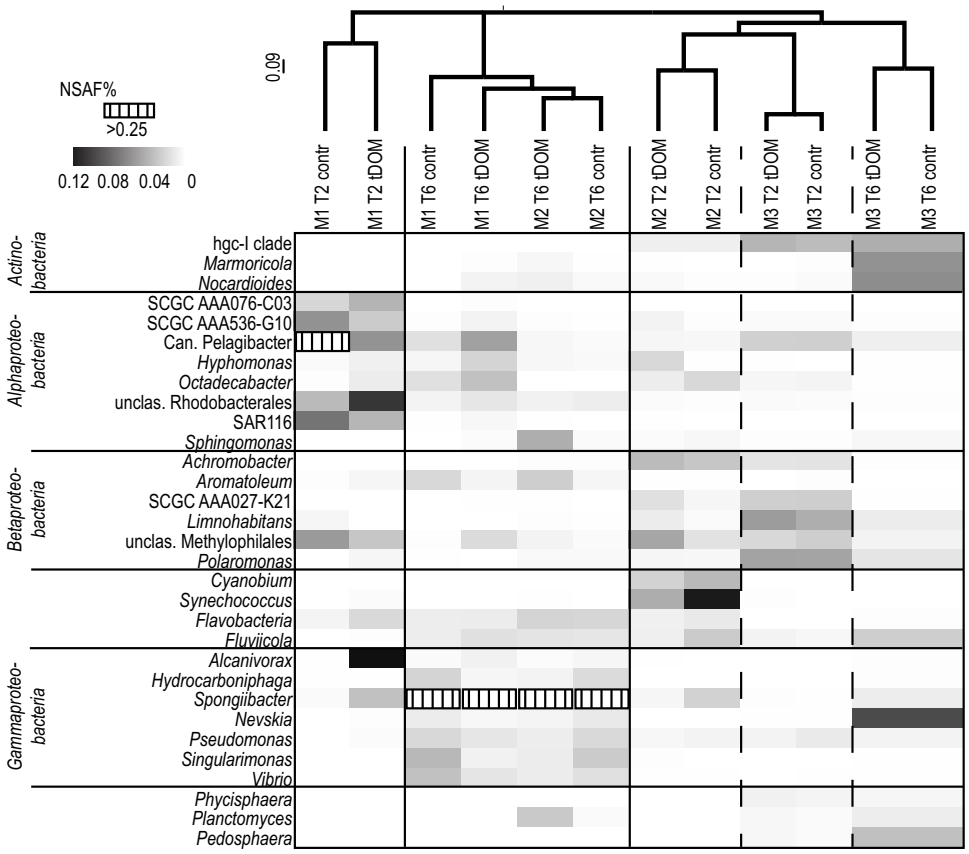

FIG 5 Relative protein abundance in abundant genera/clades in the individual enclosure experiments. M1, marine; M2, mesohaline; M3, oligohaline. The total abundances of all proteins assigned to the respective genus, expressed as normalized spectral abundance factors (NSAF%), are displayed. Only the genera that belonged to the five most abundant genera in at least one of the samples are included. T2, middle phase; T6, late phase of the incubation; contr, control (untreated); tDOM, manipulation with terrigenous carbon; SCGC, single-amplification genomes. The cluster analysis is based on the UPGMA algorithm using the Bray-Curtis similarity index. Protein abundance values were obtained from the combined database search of two independent biological replicates ($n = 2$) per sample (see Materials and Methods for details).

accompanied by a shift in the abundant metabolic functions (Fig. 4B; see also Table S4). In all enclosures and for the controls as well as for the tDOM manipulations, the relative abundances of proteins assigned to the COGs functional categories I (lipid transport and metabolism), C (energy production and conversion), and H (coenzyme transport and metabolism) were higher in P3 than in P2. Simultaneously, the relative abundances of the categories G (carbohydrate transport and metabolism) and Q (secondary metabolite biosynthesis, transport, and catabolism) were higher in P2 than in P3.

The community composition patterns determined by 16S rRNA gene analysis were mirrored by the taxonomic assignments of the total identified bacterial proteins (Fig. 5). Samples taken from the marine enclosures during P2 were dominated by proteins assigned to alphaproteobacterial genera (control [c], 71%; tDOM-treated [tDOM], 50%), particularly, the cultivated member of SAR11, "*Candidatus* Pelagibacter" (Fig. 5, Table S2, and Fig. S2). Betaproteobacterial (c, 8%; tDOM, 6%) and gammaproteobacterial (c, 5%; tDOM, 26%) proteins were also abundant. Bacterial communities in the mesohaline and oligohaline enclosures were notably more diverse during P2. In contrast to the marine enclosure, alphaproteobacterial proteins were less dominant in the mesohaline (c, 8%; tDOM, 20%), and oligohaline (c, 18%; tDOM, 17%) enclosures, where betaproteobacterial proteins were instead more abundant (mesohaline: c, 9%; tDOM, 21%; oligohaline: c, 37%; tDOM, 39%). Proteins assigned to *Cyanobacteria* were particularly abundant under mesohaline conditions in P2 (c, 16%; tDOM, 7%). In addition, during this phase and in both the mesohaline and the oligohaline enclosures, the most

abundant protein groups included actinobacterial (c, 9%; tDOM, 8%) and gammaproteobacterial (mesohaline: c, 9%; tDOM, 7%; oligohaline: c, 7%; tDOM, 9%) proteins.

Between the early phase (P2) and late phase (P3), the protein profiles in all enclosures underwent a substantial shift reflecting that in the taxonomic composition (Fig. 5; Fig. S2). A cluster analysis of protein abundance in the individual taxonomic groups (Fig. 5, top) revealed the increasing similarity of the marine and mesohaline enclosures but also showed clear differences between P2 and P3 samples. In the oligohaline enclosures, however, samples from P3 still clustered with their P2 counterparts (Fig. 5). In all enclosures, gammaproteobacterial proteins were by far the most abundant protein group during P3, accounting for 78% (c) and 48% (tDOM) of total protein abundance in the marine enclosures, 48% (c) and 43% (tDOM) in the mesohaline enclosures, and 32% (c) and 15% (tDOM) in the oligohaline enclosures (Fig. S2). Most of the gammaproteobacterial proteins during P3 were assigned to the genus *Spongiibacter*, which accounted for 57% of the total protein abundance in the control marine enclosures (34% in the marine tDOM samples) and 26.5% in the control mesohaline enclosures (tDOM, 30%) (Table S2) but only 9.2% (tDOM, 0.9%) in the oligohaline enclosures. In the latter, however, 11% (c) (tDOM, 8.5%) of the protein abundance during P3 was assigned to the gammaproteobacterial genus *Nevskia*. Additionally, in the P3 samples from the oligohaline enclosures, 18% (c) (tDOM, 25%) of the protein abundance was assigned to *Actinobacteria* and 9% (c) (tDOM, 16%) to *Betaproteobacteria*. Within the *Actinobacteria*, most proteins were assigned to members of the hgc-I clade (c, 2.5%; tDOM, 3.8%).

Although the overall protein patterns differed between the tDOM-treated and control samples, they were always more similar to each other than to those of the other enclosures. Likewise, the changes in community composition in P2 versus P3 were very similar in the tDOM and respective control samples (Fig. 5; Fig. S2).

Functional changes in abundant bacterial taxa. We combined 16S rRNA gene analyses, metagenomics, and metaproteomics. In this comprehensive and integrated approach, the individual methods and their respective advantages complemented each other, as previously demonstrated in several marine ecology studies (15–17). This procedure provided a detailed picture of taxonomy, function, and protein abundance in our samples. The common denominator was the genus-level taxonomy. While 16S rRNA gene analysis yielded estimations on the relative abundance of individual genera, the respective functions of these genera were determined on the metagenome level, and abundance of the individual functions of abundant genera was determined on the metaproteome level.

Both 16S rRNA gene analysis and metaproteomics revealed a substantial shift in the taxonomic composition during our experiments. Abundant functions within the general Clusters of Orthologous Groups (COGs) category ″metabolism″ (Fig. 6) of the identified bacterial genera were analyzed in detail. Focusing on highly abundant genera (the 2 to 5 most abundant bacterial genera derived from 16S rRNA gene analyses) rather than on the entire community is necessary, since changes in the relative abundance of the COGs categories across the bacterial community as a whole provide only a rough overview of the actual variations in relevant protein functions. This is because individual taxa may undergo opposing metabolic adaptations during an incubation, such that a function that is upregulated in one taxonomic group may simultaneously be downregulated in another. In the marine enclosures during P2, the abundant genera "*Candidatus* Pelagibacter," *Rhodobacterales* sp., *Alcanivorax* sp., and SAR116 expressed particularly high levels of ABC-type transporters of carbohydrates and amino acids as well as TRAP-type transporters of C_4 compounds (COGs categories E [amino acid transport and metabolism] and G [carbohydrate transport and metabolism]) (Fig. 6). ATP synthetases and other proteins in category C (energy production and conversion) were moderately abundant in these genera. Interestingly, the functional profile detected for the dominating genus in the P3 samples in the marine enclosures, *Spongiibacter*, was highly distinct from that of the abundant genera in P2. Thus, rather

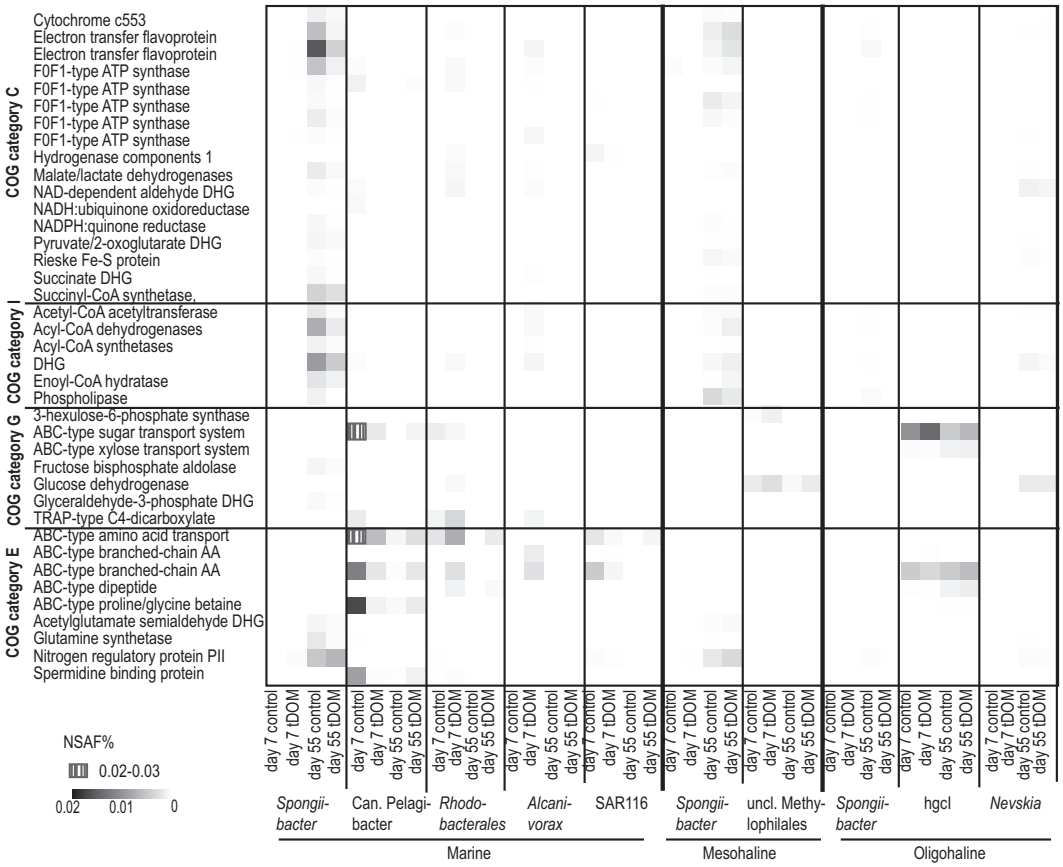

FIG 6 Relative abundance of metabolic (COGs) functions within the general COGs category "metabolism." The relative abundances of bacterial protein functions, expressed as normalized spectral abundance factors (NSAF%), are displayed for the most abundant genera. day 7, middle phase of the incubation; day 55, late phase of the incubation; DHG, dehydrogenase; tDOM, manipulation with terrigenous carbon; Can, Candidatus; uncl, uncultured. Protein abundance values were obtained from the combined database search of two independent biological replicates ($n = 2$) per sample (see Materials and Methods for details).

than ABC-type transporters, *Spongiibacter* expressed a high abundance of enzymes from the categories C (energy production and conversion; e.g., highly abundant electron-transfer flavoproteins and succinyl-CoA synthetases), I (lipid transport and metabolism; particularly, acyl coenzyme A [acyl-CoA] and other dehydrogenases), and proteins related to secondary metabolite synthesis. A similar pattern of abundant *Spongiibacter* protein functions was found in the P3 samples from the mesohaline enclosures, although the overall abundances were lower. Abundant proteins in the general COGs category "metabolism," assigned to *Methylophilales* sp. HTCC2181, particularly abundant in the P2 samples of the mesohaline enclosures, included glucose dehydrogenase and 3-hexulose-6-phosphate synthase (category G [carbohydrate transport and metabolism]). Note that most of the abundant proteins of the abundant genera in the P2 samples of the mesohaline enclosures were assigned to other general COGs categories ("information storage and processing" or "cellular processes and signaling") and were thus not included in Fig. 6.

In the oligohaline enclosures, the hgc-I clade was among the dominant taxonomic groups, and its ABC transporters from the COGs categories G (carbohydrate transport and metabolism) and E (amino acid transport and metabolism) belonged to the most abundant hgc-I clade functions in P2. Unlike *Alphaproteobacteria*, which dominated in the marine enclosures during P2 but were hardly detectable during P3, the hgc-I clade and its numerous functions were detected at similar abundances in both phases. *Spongiibacter* proteins assigned to categories I (lipid transport and metabolism) and C (energy production and conversion) were found in much lower abundances in the P3

samples from the oligohaline enclosures than in those from the marine and mesohaline enclosures. Interestingly, the P3 samples of the oligohaline enclosures featured several abundant *Nevskia* proteins that fell into these same categories (Fig. 5). *Nevskia* was the most abundant genus in the P3 oligohaline protein samples.

DISCUSSION

In this study, we investigated changes in bacterial community composition and metabolism during long-term confinement to determine whether bacteria that become dominant in such incubations have specific advantageous particularities in addition to grazing resistance. A previous study focused on DOM transformations between the early (P1) and middle (P2) phases of the experiment (13), as no significant transformations occurred during the late phase (P3) (13). Similarly, the metaproteome analysis conducted in the present study identified only a few differences in relative protein abundance between the tDOM-manipulated and control enclosures during P3. Proteins with relatively higher abundances in the tDOM-treated samples included cell surface proteins such as outer membrane receptors, porins, and certain ABC- and TRAP-type transport systems (see Table S1 in the supplemental material). However, very few of those proteins were abundant ($\geq$0.1% normalized spectral abundance factors [NSAF]), and most of the respective fold changes were low ($<$2). Overall, during P3, there was no general correlation between protein abundance patterns and the presence of tDOM. Therefore, the enrichment of *Gammaproteobacteria* (Fig. 2) in the respective enclosures appears to have been independent of the tDOM manipulation.

Cell number dynamics during the three confinement phases. Typically, over the course of a confinement in enclosure experiments, the early phase (P1) is characterized by an increase in bacterial cell numbers, the middle phase (P2) by a decrease and the development of HNAN, and the late phase (P3) by bacterial cell numbers that are close to or higher than the initial level (7) (Fig. 1). Prefiltration through the 1-μm membranes did not exclude but only reduced HNAN (18), but the use of smaller mesh sizes would have excluded larger-sized bacteria from the experiments. Nonetheless, the 1-μm prefiltration successfully delayed HNAN development for approximately 1 week.

A high abundance of HNA cells in P1 and their decline during P2 characterized both the mesohaline and the marine enclosures but not the oligohaline enclosures (Fig. 1). The specific predation of HNA cells by HNAN grazers is typical of incubation experiments (2, 19, 20). In previous studies, the prey size-dependent feeding behavior of HNAN and their higher grazing rates on active than on inactive bacteria were described (21). In all oligohaline enclosures of this study, LNA cells were more abundant than HNA cells, but a peak in the number of grazers comparable to that in the marine enclosures was observed. This suggested that the LNA bacterial community in the oligohaline confinements comprised active bacterial groups with permanently small cells, such as hgc-I (22, 23), that were less successfully grazed upon by HNAN. However, the temporal resolution for grazers in this study was relatively low, and some aspects of HNAN population dynamics may have been missed.

Shift in the bacterial community composition between P2 and P3. The metaproteomic and 16S rRNA gene analyses showed that the microbial communities in the P2 enclosures consisted mostly of the representatives typically found at similar salinities in the Baltic Sea and other estuaries (Fig. 3 and 5; Table S1). For example, *Alphaproteobacteria* such as "*Candidatus* Pelagibacter," *Roseobacter*, and members of the SAR116 clade are abundant in marine regions of the Baltic Sea (24, 25). In line with these findings, the abundance of *Alphaproteobacteria* in our data set was higher under marine than under mesohaline or oligohaline conditions, while the abundances of cI500-29 OTU and hgc-I (both *Actinobacteria*) as well as *Limnohabitans* and *Polaromonas* (both *Betaproteobacteria*) were highest under oligohaline and lowest under marine conditions (Fig. 3). In the late phase of the marine and mesohaline enclosures, the proportion of proteins and 16S rRNA genes assigned to *Gammaproteobacteria* increased substantially, whereas the abundances of 16S rRNA genes and proteins assigned to *Alphaproteobacteria* and *Betaproteobacteria* decreased. In the oligohaline

enclosures, the actinobacterial hgc-I clade continuously dominated the 16S rRNA genes, and its genera were the most abundant among those detected in our metaproteome analysis, in both P2 and P3. A shift in the bacterial community composition (Fig. 2 and 3) of marine and mesohaline enclosures toward *Gammaproteobacteria* has been observed in many other marine confinement experiments (3, 5, 19, 26), although the gammaproteobacterial families dominating an enclosure will depend on the sample source. Thus, Stewart et al. (6) and Müller et al. (27) reported the dominance of *Colwelliaceae*, whereas Sipler et al. (28) found mostly *Oceanospirillaceae*. Significant increases in *Moraxellaceae* (4) and *Pseudoalteromonadaceae* (29) have been reported from Baltic Sea enclosure experiments. Interestingly, in a confinement experiment using lake water, *Flavobacterium* was the dominant genus (30), whereas in the oligohaline enclosures of our experiment, members of the *Actinobacteria* dominated. The gammaproteobacterium *Spongiibacter* was also present in our experiment under oligohaline conditions but at much lower abundances. *Spongiibacter marinus*, the cultivated representative closest to our spongiibacterial 16S rRNA sequence, tolerates a salinity between 7 and 70 g NaCl/liter (14). Thus, under oligohaline conditions (salinity 3), *Spongiibacter* may be outside its salinity range. This suggests that physiological limitations, such as the salinity range, impact the bacterial community, which supports the hypothesis that the "bottle effect" is a biological phenomenon rather than a physical effect attributable to the size and/or type of the enclosure. However, salinity may also influence the composition of bacterial grazers, which, in enclosure experiments, have a substantial effect on the bacterial community (5, 8). While grazers usually feed relatively nonspecifically on active cells (see above), high grazing rates result in the emergence of "grazing-resistant" bacterial communities (7). In accordance with this observation, *Spongiibacter* was shown to be relatively grazing resistant (31). Grazing resistance has also been attributed to the actinobacterial hgc-I clade, mainly due to its smaller than average cell size (22, 23) and potentially also due to the composition of its cell wall and/or its surface properties (32). Our results therefore support previous studies concluding that grazing resistance is essential for long-term survival during confinement.

Putative metabolism of abundant bacteria in the late phase of the experiment. The taxonomic assignment of the proteins detected in the metaproteome was in good accordance with the changes observed in the 16S rRNA gene analysis (Fig. 3 and 5). The most abundant bacterial genera determined by these two methods were examined with regard to their individual functions as revealed by the metaproteome analysis. Metaproteome analyses are excellent tools to investigate the specific physiological activity of microbial communities, as they circumvent the limitations of cultivation-based methods and, in contrast to metagenomics, also provide information on protein abundance (33). While metaproteomics may not always be able to distinguish between very similar proteins of the same function from closely related species or genera, the combination with 16S rRNA data compensates for this potential drawback. Knowledge on dominant genera, as obtained from 16S rRNA analyses, allowed us to assign metaproteomics-derived protein functions specifically to individual genera. This approach has been successfully applied previously (15–17). Assignment of protein functions to taxonomic groups is crucial when analyzing metabolic processes in microbial communities, since thousands of taxa contribute proteins with overlapping functions in an environmental sample. Increased abundance of some functions may thus be accompanied by decreased abundance of others in the same category, as shown to occur during exponential and stationary growth phases (34). We focused on the most abundant bacterial taxa to identify the metabolic particularities of organisms in P3 versus P2 (Fig. 5).

The succession of different bacterial groups in confinement experiments, i.e., the total demise of some and the decrease of others, is also a function of the presence of bioavailable nutrients and carbon. High-affinity transporters from the COGs categories G (carbohydrate transport and metabolism) and E (amino acid transport and metabolism) were among the most abundant functions detected for "*Candidatus* Pelagibacter"

(belonging to SAR11) and other abundant *Alphaproteobacteria* in the marine enclosures during P2 (Fig. 5). Previous studies showed that, upon incubation in the dark, "*Candidatus* Pelagibacter" cells upregulate genes for amino acid transport (35). The genome of "*Candidatus* Pelagibacter" encodes a large number of high-affinity transporters that, under oligotrophic conditions, are expressed at disproportionally higher abundances than other species of bacteria (36, 37). While a similar result was obtained during P2 in our study, the abundance of "*Candidatus* Pelagibacter" decreased in P3 (Fig. 6), despite the fact that the bacterium is not primarily targeted by HNAN (38). High-affinity ABC-type transporters for sugars and branched-chain amino acids were also highly abundant in hgc-I under oligohaline conditions (Fig. 6). However, in contrast to those of "*Candidatus* Pelagibacter," the ABC transporters of hgc-I were still abundant in the 55-day sample. In our enclosure experiments, the organic carbon (e.g., humic acids [13]) in the 55-day samples was relatively recalcitrant. Therefore, bacteria abundant in P3 must either make the recalcitrant DOM resources accessible or find an alternative carbon supply for survival. There is no evidence that members of SAR11 are able to use recalcitrant carbon. In contrast, the strong genetic potential of members of the actinobacterial hgc-I to metabolize carbohydrate- and N-rich organic compounds as well as polysaccharides has been reported (39, 40). Moreover, hgc-I is found in high abundance in humic acid-rich freshwater habitats (41). These findings suggest that hgc-I was able to use the recalcitrant tDOM present in the 55-day samples.

Enzymes for the utilization of recalcitrant carbon are not known for *Spongiibacter*. It is therefore very likely that, in contrast to hgc-I, this organism could not use the recalcitrant carbon available in the enclosures during P3. Metaproteome analysis revealed that *Spongiibacter*'s most abundant proteins belonged to "electron transfer flavoproteins" (COGs category F), which are also involved in the β-oxidation of lipids and the transfer of two electrons from acyl-CoA dehydrogenase to cytochromes (Fig. 6). In the P3 samples, acyl-CoA dehydrogenase and acetyl-CoA acetyltransferases (COGs category I [lipid metabolism]) were also among the abundant *Spongiibacter* proteins, as were an apolipoprotein and a phospholipase, both of which contribute to the degradation of fatty acids. The low-level bacterial activity previously measured in P3 (13) indicated that the bacteria present during this phase of the experiment were for the most part inactive. However, many bacteria can reroute their internal metabolism to respond to limitations in the energy supply and mobilize alternative nutrient sources to survive in a low-activity status. Besides internal stores of polyphosphates, components of the cellular machinery can be catabolized to provide nutrients. Both mechanisms have been demonstrated in gammaproteobacterial model organisms. In *Escherichia coli*, for example, a derepression of genes involved in β-oxidation and fatty acid degradation is required for long-term survival (42). *Vibrio cholerae* substantially reduces its pool of total lipids (43), and carbon-starved *Vibrio harveyi* is known to upregulate fatty acid β-oxidation so as to facilitate the use of membrane phospholipids as an endogenous energy source (44). Our data indicate similar metabolic responses in *Spongiibacter*, evidenced by the high abundance of acetyl-CoA-associated proteins during P3 and the presence of components of the glyoxylate shunt, an anaplerotic pathway that bypasses the citrate cycle in the biosynthesis of precursors. These results may suggest that *Spongiibacter* uses cell wall components as an endogenous energy source allowing survival during long-term incubations. This may also be true for *Nevskia* in the oligohaline enclosures, where similar protein expression patterns were recorded.

Spongiibacter is almost absent in the natural bacterial community of the Baltic Sea and was barely detectable in the enclosures at the start of our experiment. However, by P3, *Spongiibacter* had outcompeted most other bacteria (Fig. 3), particularly in the marine enclosures (Fig. 6). As revealed by our 16S rRNA analysis, the P3 samples were dominated by a *Spongiibacter* species, which showed 93% identity (on 16S rRNA gene level) to *Spongiibacter marinus* DSM 19753. In light of this close phylogenetic relatedness, it is reasonable to assume that both species are metabolically highly similar. With the *S. marinus* DSM 19753 genome available (NCBI accession NZ_AULP00000000.1), we were thus able to evaluate the physiological potential of the abundant *Spongiibacter* in

our enclosures. A screening for secondary metabolite synthesis genes (antiSMASH [45]) in the *S. marinus* DSM 19753 genome detected 68 genes, arranged in four gene clusters, which encode enzymes involved in the synthesis of metabolites such as bacteriocin and nonribosomal peptides (see Table S5A). Mapping of these genes to the M1 metaproteome of this study revealed 143 matches with pronounced similarities (E values $< 1e^{-15}$, bitscores > 80) among the identified proteins of various genera in the marine enclosures, including 53 *Spongiibacter* proteins (Table S6). Nine of the detected *Spongiibacter* proteins in the marine enclosure matched to *S. marinus* DSM 19753 genes with predicted "core biosynthetic" functions in the production of the above-mentioned secondary metabolites. The relative abundance of these proteins accounted for 0.33% NSAF of all identified proteins in control samples at day 55 (while they were not detected at all at day 7) (Table S5B).

In light of the high *Spongiibacter* abundance observed in P3, this might indicate that the dominant *Spongiibacter* species in our samples produce secondary metabolites that enhance its competitiveness during the incubation. Ribosomally synthesized bacteriocins and nonribosomally synthesized peptides are potent bioactive compounds. Gram-negative bacteriocins can have antibacterial pore-forming activity as well as nuclease and muramidase activities (46). Nonribosomal peptides reveal versatile antimicrobial activities (47–49). Thus, the identification of related *Spongiibacter* genes in our metagenome data sets and detection of the respective proteins in our metaproteome samples indicate an active role of such bioactive peptides in these long-term cultivations. However, as the presence of secondary metabolism-related genes may vary between species within the same genus (50–52), this hypothesis will need to be evaluated in future studies.

Our results indicate that besides grazing, other less-appreciated factors are important in determining bacterial community succession during long-term incubations, including the initial bacterial community composition, alternative bacterial strategies to acquire carbon in the absence of labile carbon sources, and the putative ability to produce antimicrobial substances. Microbiologists conducting long-term experiments, especially in the absence of continuous labile carbon addition (as in chemostats), are thus confronted with the fundamental problem that some bacteria are "genetically privileged" during long-term incubations. The physiological characteristics of the initial microbial community, such as the ability to use internal carbon sources and synthesize bioactive substances, may substantially affect the outcome of the manipulation. Our results strongly emphasize the need for new strategies in enclosure experiments with complex bacterial communities, such as short-term experiments in which metabolic responses are directly monitored during the incubations using -omics tools, or through sophisticated, less biased experimental setups such as flowthrough chambers (30).

MATERIALS AND METHODS

Enclosure experiments. The setup of the enclosures is described in detail by Herlemann et al. (13). In brief, water from the Kalix River was collected close to Svartbyn, Sweden (66°15′26.97′′N, 22°49′28.38′′E) on 3 June 2011, immediately filtered through a 0.2-μm mesh (polypropylene, GR22-PFG-110; MTS, Bad Liebenzell, Germany) and stored at −20°C. For the enclosure experiments, the Kalix water was thawed and added as the terrigenous dissolved organic matter (tDOM)-rich manipulation. The enclosures were set up using surface water obtained from three stations, representing marine (salinity 32 [M3]; Kattegat/Skagerrak, 58°07,998′N, 10°00,000′E), mesohaline (salinity 7 [M2]; Baltic Proper, 57°18,342′N, 20 04,692′E), and oligohaline (salinity 3 [M3]; Bothnian Bay, 65°26,700′N, 23°17,898′E) conditions, during a cruise of the R/V *Meteor* in May 2012. After filtration of the seawater samples through 100-μm gauze and a 1-μm mesh (polypropylene, TAX1-10; MTS, Bad Liebenzell, Germany), 60 liters was transferred to each of three 120-liter polypropylene tanks. Two of the tanks contained 60 liters of thawed 0.2-μm filtered Kalix water, in which the salinity was already adapted to the *in situ* salinity of the station by the addition of 100×-enriched artificial seawater (for details of the composition, see reference 4), referred to as tDOM. Instead of Kalix river water, the control tank (c) contained 60 liters of 1-μm-prefiltered Baltic Sea water and 60 liters of 0.2-μm-filtered (polypropylene filters, GR22-PFG-110; MTS, Bad Liebenzell, Germany) Baltic Sea water. The total nitrogen (N) and phosphorus (P) concentrations in all tanks were adjusted to 10 μM NO_3NH_4 and 1 μM $NaHPO_4$, respectively, to avoid N and P limitations during the experiment. After the salinity had been adjusted, the t0 (start) samples were taken and the water remaining in each tank was distributed in three replicate 25-liter polyethylene carboys, which were then held at a constant temperature of 10°C in dark climate chambers. Samples were obtained at t0 and

after 2, 7, 13, and 55 days (not every parameter was measured at each time point). All nonglass materials were rinsed before use, first with ultrapure water and then several times with sample water. For an overview of all samples and replicate numbers in this study, see Table S7 in the supplemental material.

Flow cytometry. For bacterial enumeration, 4-ml subsamples were fixed for 1 h with 400 μl of 1% paraformaldehyde and 0.5% glutaraldehyde, shock frozen in liquid nitrogen, and stored at −80°C until processed by flow cytometry. Samples were measured on a FacsCalibur (Becton, Dickinson) using a modification of the method described by Gasol et al. (53). Briefly, after the addition of 0.2-μm-filtered SYBR green solution (2.4 M potassium citrate, 0.2 M dimethyl sulfoxide, and 5 μl SYBR green) to 300 μl of the sample, the mixture was incubated for 30 min in the dark and then subjected to flow cytometry at a medium previously determined flow rate. The flow diagrams were evaluated using the software CellQuestPro. Based on size and fluorescence, two populations were distinguished: high-nucleic acid (HNA) cells and low-nucleic acid (LNA) cells.

Samples for the enumeration of heterotrophic and autotrophic nanoplankton (HNAN $<$ 10 μm) were preserved with formaldehyde (2% final concentration), filtered through 0.8-μm black polycarbonate filters (Whatman), and stained for 1 min with 4′,6-diamidino-2-phenylindole (DAPI; final concentration, 2 μg/ml). At least 30 cells per filter were counted at 630× amplification using an Axioskop 2 epifluorescence microscope (Carl Zeiss MicroImaging, Germany).

Bacterial community composition. To exclude aggregates and particle-associated organisms, water samples (1 liter) for DNA analysis were filtered first through 5-μm filters and then through 0.2-μm-pore-size white polycarbonate filters (13). The DNA of the 0.2-μm fractions was extracted according to the method described by Weinbauer et al. (54). 16S rRNA gene sequences were amplified using the protocol described by Herlemann et al. (24). Briefly, the DNA was PCR amplified using the primers Bakt_341F and Bakt_805R and 30 cycles of amplification. The amplicons were purified using Agencourt AMPure XP (Becker Coulter) and sent for 454 pyrosequencing, using Roche GS FLX 454 Titanium series chemistry, to Eurofins MWG Operon (Ebersberg, Germany).

The resulting sequences were quality-checked by RDPpyro (55) with the following settings: maximum number of N, 0; minimum sequence length, 50; and minimum exponential Q-score, 20. They were then evaluated using the SILVA next-generation sequencing (NGS) pipeline based on SILVA release version 119 (56). SILVA NGS performs additional quality checks based on SINA (57) alignments with a curated SEED database and rejects problematic reads such as PCR artifacts and 16S rRNA sequences. The quality settings in SILVA NGS were maximum ambiguities of 2%, maximum homopolymers of 2%, and a minimum alignment score of 40. For each operational taxonomic unit (OTU), the longest read served as a reference for taxonomic classification in a BLAST (version 2.2.28+) search against the SILVA SSURef data set. The resulting classification of the reference sequence was mapped to all members of the respective OTU. Sequences having an average BLAST alignment coverage and alignment identity of $<$93% were defined as unclassified. Resulting sequences had an average length of 458 bp, and the sequencing depth did not reach a clear saturation. The original run contained 484,499 sequence reads; the subset used in this analysis included 175,925 sequence reads that were sum-normalized prior to the analysis. Sequences present only once in the entire data set (singletons) were excluded, as were those assigned to "chloroplasts" and *Archaea*, since the primer set used in this study has only a limited coverage of these groups. The 16S sequences were classified to the genus level, and lineages without a defined genus were assigned on the next defined level. Bacterial community compositions at each time point and treatment were visualized using nonmetric multidimensional scaling (NMDS) based on Bray-Curtis dissimilarity. A complementary canonical correspondence analysis (CCA) showed that time and salinity were the most important factors for determining the bacterial community composition (see Fig. S3), and consequently, these environmental parameters were added to the NMDS plot *post hoc*.

Metagenome analysis. Samples for metagenome and proteomic analyses were obtained by filtering 2.5 liters of water from each enclosure onto 0.2-μm filter discs (12 cm) using a peristaltic pump and then freezing the filters at −80°C until DNA/protein extraction. A total of 17 metagenomes were generated. DNA was extracted from the filters that were also used for the metaproteome analysis (see below). DNA was sheared, size-selected, and subjected to library construction using the Nextera XT DNA library prep kit, according to the manufacturer's protocols (Illumina). It was then clustered using cBot and sequenced on HiSeq 2500 with a 2 × 101 setup in HighOutput mode. Bcl to Fastq conversion was performed using bcl2Fastq v1.8.3 from the CASAVA software suite (Sequencing analysis software user guide for pipeline version 1.3 and CASAVA version 1.0; Illumina Inc., San Diego, CA, USA). The quality scale was Sanger/phred33/Illumina1.8+. The sequencing reads were quality trimmed using the sickle function with a quality setting of 20. The reads for each sample were assembled separately with Ray (58) using a kmer of 31 and then mapped back using bowtie2 (59) and default parameters. PCR duplicates were removed using bowtie2, and coverage was determined using BEDTools (60). The script used for mapping is available at github: https://github.com/inodb/metassemble/blob/master/scripts/map/map-bowtie2-markduplicates.sh. The assembled contigs were uploaded to IMG/MER and automatically annotated (61) under the following IMG genome identifiers (IDs): 3300002224, 3300002230, 3300002227, 3300002226, 3300002131, 3300002144, 3300002132, 3300002137, 3300002140, 3300002142, 3300002136, 3300002134, 3300002139, 3300002141, 3300002138, and 3300002143 (see Table S8 for details). IMG/MER was used to investigate the function and putative operon structure of the genes of interest. The functions and taxonomy of all protein-coding genes in the metagenomes were predicted by automatic annotation in the IMG pipeline (61) (see above). For additional functional characterization, the amino acid sequences of all identified proteins were subjected to a local BLAST search (BLAST-2.7.1+ [62]) against the transporter classification database (TCDB) (63) to identify and classify transporters (E value threshold, 10^{-6}). In addition, Clusters of Orthologous Groups (COGs) identifiers were assigned to all identified

proteins using a local rps-BLAST search against the Conserved Domain Database (CDD; E value threshold, 10^{-5} [64]) to classify protein functions into metabolic categories. The *Spongiibacter marinus* DSM 19753 genome (NCBI accession NZ_AULP00000000.1) was screened for secondary metabolite synthesis gene clusters using antiSMASH (45) at default settings.

Protein database construction. Translation and open reading frame (ORF)-finding were automatically performed in IMG to create amino acid sequence files in .faa format. All acquired amino acid sequences of the same sampling site were combined into comprehensive site-specific protein database files: marine site (M1), 4 metagenomes; mesohaline site (M2), 7 metagenomes; oligohaline site (M3), 5 metagenomes (see Table S8 for details on the metagenomes included in the respective protein databases). Redundant sequences were removed using CD-Hit (65) at 100% identity. For protein identification, the site-specific protein databases were complemented by reversed sequences of all proteins (decoys, to allow for the determination of false discovery rates) and a set of common laboratory contaminants.

Protein extraction and preparation for mass spectrometry. Samples for metaproteomic analyses were obtained as described above for metagenomic samples, and the proteins were extracted from the filtered samples as described by Teeling et al. (16), with minor modifications: one-half of each frozen filter was used for the analyses. Filter halves were cut into small pieces and transferred to 1.8-ml tubes containing lysis buffer (50 mM Tris, 2% SDS, 10% glycerol, 0.1 M dithiothreitol [DTT], pH 6.8) and 180-μm glass beads. Cells on the filter pieces were disrupted by bead beating in a bead mill (3×30 s, 6.5 m/s, 5-min pause at 4°C between runs). After pelleting of the beads and filter pieces by centrifugation ($15,500 \times g$ for 4 min at 4°C), the supernatants (i.e., protein raw extracts) were subjected to ultracentrifugation ($100,000 \times g$ for 1 h at 4°C). The resulting supernatants (i.e., enriched soluble proteins devoid of cell membranes and debris) were precipitated in ice-cold acetone at −20°C for 16 h. The proteins were pelleted ($15,500 \times g$ for 10 min at 4°C), washed in 96% ethanol, and dried in a vacuum centrifuge. For SDS-PAGE, the protein pellets were gently resuspended in sample buffer (0.1 M Tris-HCl [pH 6.8], 10% SDS, 20% glycerol, 5% mercaptoethanol, bromophenol blue), denatured (10 min at 90°C) and loaded onto precast mini gels (Bio-Rad TGX, 4% to 20%). After electrophoresis (50 min at 150 V), the gels were stained with Coomassie brilliant blue (G250; Sigma-Aldrich) for 16 h and then washed in double-distilled water to remove excess stain. Protein lanes excised from the gels were divided into 10 equal-sized pieces (subsamples) per sample and destained (200 mM NH_4HCO_3, 30% acetonitrile), and the proteins were then in-gel digested at 37°C for 16 h using trypsin solution (sequencing-grade modified trypsin, 1 μg/ml; Promega) (66). The resulting peptides were purified using ZipTip pipette tips (Millipore) according to the manufacturer's instructions.

ESI-MS/MS measurements and semiquantitative data analysis. Electrospray ionization tandem mass spectrometry (ESI-MS/MS) measurements, data filtering, and analysis were performed as recently described by Ponnudurai et al. (67). Briefly, peptide mixes were separated in a nano-high-performance liquid chromatography (nano-HPLC) system (Easy-nLCII HPLC; Thermo Fisher Scientific) followed by MS/MS analysis in an LTQ Orbitrap Velos mass spectrometer (Thermo Fisher Scientific). All MS/MS spectra were searched against the respective sampling site-specific target-decoy metaproteome database, i.e., samples taken at the marine site (M1) were searched against the M1 database, those from the mesohaline site against the mesohaline enclosure (M2) database, etc., using the SORCERER system (SageN, Milpitas, CA, USA) with the integrated SEQUEST algorithm (version 27, revision 11; Thermo Fisher Scientific, San Jose, CA, USA). The resulting protein identifications were filtered and analyzed with Scaffold (version 4.0.6.1; Proteome Software Inc., Portland, OR). Protein identifications were accepted if they had a minimum of two identified peptides and passed the following "sequest" filter: XCorr for doubly charged peptides, 2.2; for triply charged peptides, 3.3; and for quadruply charged peptides, 3.8; delta correlation score, 0.1 (68). Total spectral counts were used to calculate relative protein abundances for each of the identified proteins as the percent normalized spectral abundance factors (NSAF) (69). All protein abundance values mentioned in the text refer to NSAF%, i.e., a protein's abundance relative to all proteins in the same sample, even if—for readability's sake—they are given as a percentage. Two biological replicates of each sample were measured independently ($n = 2$). The resulting spectra of both replicates were combined for the database search. Spectral counts and protein abundance values are therefore not given for individual replicates but for the entire sample, i.e., for the combination of both replicates. Although this prevents the determination of average values (and standard deviations), the combined database search allows for increased protein identification rates, and protein abundance values derived from the pooled spectra are representative of two independent samples. While label-free proteomics is semiquantitative (and does not provide absolute protein abundances), comparing relative protein abundances across different samples allows for solid monitoring of differences in protein abundance.

Data availability. The sequences from bacterial amplicons were deposited under European Nucleotide Archive accession number PRJEB7141. The mass spectrometry proteomics data were deposited in the ProteomeXchange Consortium via the PRIDE (70) partner repository with the data set identifier PXD011160.

SUPPLEMENTAL MATERIAL

Supplemental material for this article may be found at https://doi.org/10.1128/AEM.00825-19.

SUPPLEMENTAL FILE 1, PDF file, 5.5 MB.

ACKNOWLEDGMENTS

This study was financially supported by the SAW-funded ATKiM project, which provided funds to D. P. R. Herlemann, C. Meeske, K. Jürgens, S. Markert, and T. Schweder. D. P. R. Herlemann was also supported by the European Regional Development Fund/Estonian Research Council funded Mobilitas Plus Top Researcher grant MOBTT24.

We thank the crew and captain of the RV *Meteor* (M86, M87) for support during the research cruise. The computations were performed on resources provided by the Swedish National Infrastructure for Computing (SNIC) at the PDC Centre for High Performance Computing (PDC-HPC) and Uppsala Multidisciplinary Center for Advanced Computational Science (UPPMAX). We thank Jana Matulla for excellent technical assistance and Stephan Fuchs for his help and advice in MS database construction. We also thank Stefan E. Heiden for valuable help with the CDD BLAST analyses.

REFERENCES

1. Duarte CM, Gasol JM, Vaqué D. 1997. Role of experimental approaches in marine microbial ecology. Aquat Microb Ecol 13:101–111. https://doi.org/10.3354/ame013101.
2. Eilers H, Pernthaler J, Amann R. 2000. Succession of pelagic marine bacteria during enrichment: a close look at cultivation-induced shifts. Appl Environ Microbiol 66:4634–4640. https://doi.org/10.1128/AEM.66.11.4634-4640.2000.
3. Fuchs BM, Zubkov MV, Sahm K, Burkill PH, Amann R. 2000. Changes in community composition during dilution cultures of marine bacterioplankton as assessed by flow cytometric and molecular biological techniques. Environ Microbiol 2:191–201. https://doi.org/10.1046/j.1462-2920.2000.00092.x.
4. Herlemann DPR, Manecki M, Meeske C, Pollehne F, Labrenz M, Schulz-Bull D, Dittmar T, Jürgens K. 2014. Uncoupling of bacterial and terrigenous dissolved organic matter dynamics in decomposition experiments. PLoS One 9:e93945. https://doi.org/10.1371/journal.pone.0093945.
5. Massana R, Jürgens K. 2003. Composition and population dynamics of planktonic bacteria and bacterivorous flagellates in seawater chemostat cultures. Aquat Microb Ecol 32:11–22. https://doi.org/10.3354/ame032011.
6. Stewart FJ, Dalsgaard T, Young CR, Thamdrup B, Revsbech NP, Ulloa O, Canfield DE, DeLong EF. 2012. Experimental incubations elicit profound changes in community transcription in OMZ bacterioplankton. PLoS One 7:e37118. https://doi.org/10.1371/journal.pone.0037118.
7. Jürgens K, Güde H. 1994. The potential importance of grazing-resistant bacteria in planktonic systems. Mar Ecol Prog Ser 112:169–188. https://doi.org/10.3354/meps112169.
8. Schäfer H, Servais P, Muyzer G. 2000. Successional changes in the genetic diversity of a marine bacterial assemblage during confinement. Arch Microbiol 173:138–145. https://doi.org/10.1007/s002039900121.
9. Pernthaler J, Amann R. 2005. Fate of heterotrophic microbes in pelagic habitats: focus on populations. Microbiol Mol Biol Rev 69:440–461. https://doi.org/10.1128/MMBR.69.3.440-461.2005.
10. Fogg G, Calvario-Martinez O. 1989. Effects of bottle size in determinations of primary productivity by phytoplankton. Hydrobiologia 173:89–94. https://doi.org/10.1007/BF00015518.
11. Hammes F, Vital M, Egli T. 2010. Critical evaluation of the volumetric "bottle effect" on microbial batch growth. Appl Environ Microbiol 76:1278–1281. https://doi.org/10.1128/AEM.01914-09.
12. Zobell CE, Anderson DQ. 1936. Observations on the multiplication of bacteria in different volumes of stored sea water and the influence of oxygen tension and solid surfaces. Biol Bull 71:324–342. https://doi.org/10.2307/1537438.
13. Herlemann DPR, Manecki M, Dittmar T, Jürgens K. 2017. Differential responses of marine, mesohaline and oligohaline bacterial communities to the addition of terrigenous carbon. Environ Microbiol 19:3098–3117. https://doi.org/10.1111/1462-2920.13784.
14. Jang GI, Hwang CY, Choi H-G, Kang S-H, Cho BC. 2011. Description of *Spongiibacter borealis* sp. nov., isolated from Arctic seawater, and reclassification of *Melitea salexigens* Urios et al. 2008 as a later heterotypic synonym of *Spongiibacter marinus* Graeber et al. 2008 with emended descriptions of the genus *Spongiibacter* and *Spongiibacter marinus*. Int J Syst Evol Microbiol 61:2895–2900. https://doi.org/10.1099/ijs.0.028795-0.
15. Kappelmann L, Krüger K, Hehemann J-H, Harder J, Markert S, Unfried F, Becher D, Shapiro N, Schweder T, Amann RI. 2018. Polysaccharide utilization loci of North Sea *Flavobacteriia* as basis for using SusC/D-protein expression for predicting major phytoplankton glycans. ISME J 1:76–91. https://doi.org/10.1038/s41396-018-0242-6.
16. Teeling H, Fuchs BM, Becher D, Klockow C, Gardebrecht A, Bennke CM, Kassabgy M, Huang S, Mann AJ, Waldmann J, Weber M, Klindworth A, Otto A, Lange J, Bernhardt J, Reinsch C, Hecker M, Peplies J, Bockelmann FD, Callies U, Gerdts G, Wichels A, Wiltshire KH, Glöckner FO, Schweder T, Amann R. 2012. Substrate-controlled succession of marine bacterioplankton populations induced by a phytoplankton bloom. Science 336:608–611. https://doi.org/10.1126/science.1218344.
17. Unfried F, Becker S, Robb CS, Hehemann J-H, Markert S, Heiden SE, Hinzke T, Becher D, Reintjes G, Krüger K, Avcı B, Kappelmann L, Hahnke RL, Fischer T, Harder J, Teeling H, Fuchs B, Barbeyron T, Amann RI, Schweder T. 2018. Adaptive mechanisms that provide competitive advantages to marine bacteroidetes during microalgal blooms. ISME J 12:2894. https://doi.org/10.1038/s41396-018-0243-5.
18. Weber F, del Campo J, Wylezich C, Massana R, Jürgens K. 2012. Unveiling trophic functions of uncultured protist taxa by incubation experiments in the brackish Baltic Sea. PLoS One 7:e41970. https://doi.org/10.1371/journal.pone.0041970.
19. Baltar F, Palovaara J, Unrein F, Catala P, Horňák K, Šimek K, Vaqué D, Massana R, Gasol JM, Pinhassi J. 2016. Marine bacterial community structure resilience to changes in protist predation under phytoplankton bloom conditions. ISME J 10:568–581. https://doi.org/10.1038/ismej.2015.135.
20. Neuenschwander SM, Pernthaler J, Posch T, Salcher MM. 2015. Seasonal growth potential of rare lake water bacteria suggest their disproportional contribution to carbon fluxes. Environ Microbiol 17:781–795. https://doi.org/10.1111/1462-2920.12520.
21. del Giorgio PA, Gasol JM, Vaqué D, Mura P, Agustí S, Duarte CM. 1996. Bacterioplankton community structure: protists control net production and the proportion of active bacteria in a coastal marine community. Limnol Oceanogr 41:1169–1179. https://doi.org/10.4319/lo.1996.41.6.1169.
22. Pernthaler J, Posch T, Simek K, Vrba J, Pernthaler A, Glöckner FO, Nübel U, Psenner R, Amann R. 2001. Predator-specific enrichment of actinobacteria from a cosmopolitan freshwater clade in mixed continuous culture. Appl Environ Microbiol 67:2145–2155. https://doi.org/10.1128/AEM.67.5.2145-2155.2001.
23. Salcher MM, Pernthaler J, Posch T. 2010. Spatiotemporal distribution and activity patterns of bacteria from three phylogenetic groups in an oligomesotrophic lake. Limnol Oceanogr 55:846–856. https://doi.org/10.4319/lo.2010.55.2.0846.
24. Herlemann DPR, Labrenz M, Jürgens K, Bertilsson S, Waniek JJ, Andersson AF. 2011. Transitions in bacterial communities along the 2000 km salinity gradient of the Baltic Sea. ISME J 5:1571–1579. https://doi.org/10.1038/ismej.2011.41.
25. Herlemann DPR, Lundin D, Andersson AF, Labrenz M, Jürgens K. 2016.

Phylogenetic signals of salinity and season in bacterial community composition across the salinity gradient of the Baltic Sea. Front Microbiol 7:1883. https://doi.org/10.3389/fmicb.2016.01883.
26. Massana R, Pedrós-Alió C, Casamayor EO, Gasol JM. 2001. Changes in marine bacterioplankton phylogenetic composition during incubations designed to measure biogeochemically significant parameters. Limnol Oceanogr 46:1181–1188. https://doi.org/10.4319/lo.2001.46.5.1181.
27. Müller O, Seuthe L, Bratbak G, Paulsen ML. 2018. Bacterial response to permafrost derived organic matter input in an arctic fjord. Front Mar Sci 5:263. https://doi.org/10.3389/fmars.2018.00263.
28. Sipler RE, Kellogg CT, Connelly TL, Roberts QN, Yager PL, Bronk DA. 2017. Microbial community response to terrestrially derived dissolved organic matter in the coastal arctic. Front Microbiol 8:1018. https://doi.org/10.3389/fmicb.2017.01018.
29. Dinasquet J, Kragh T, Schrøter ML, Søndergaard M, Riemann L. 2013. Functional and compositional succession of bacterioplankton in response to a gradient in bioavailable dissolved organic carbon. Environ Microbiol 15:2616–2628. https://doi.org/10.1111/1462-2920.12178.
30. Ionescu D, Bizic-Ionescu M, Khalili A, Malekmohammadi R, Morad MR, De Beer D, Grossart H-P. 2015. A new tool for long-term studies of POM-bacteria interactions: overcoming the century-old bottle effect. Sci Rep 5:14706. https://doi.org/10.1038/srep14706.
31. Gong J, Qing Y, Zou S, Fu R, Su L, Zhang X, Zhang Q. 2016. Protist-bacteria associations: *Gammaproteobacteria* and *Alphaproteobacteria* are prevalent as digestion-resistant bacteria in ciliated protozoa. Front Microbiol 7:498. https://doi.org/10.3389/fmicb.2016.00498.
32. Tarao M, Jezbera J, Hahn MW. 2009. Involvement of cell surface structures in size-independent grazing resistance of freshwater *Actinobacteria*. Appl Environ Microbiol 75:4720–4726. https://doi.org/10.1128/AEM.00251-09.
33. Verberkmoes NC, Russell AL, Shah M, Godzik A, Rosenquist M, Halfvarson J, Lefsrud MG, Apajalahti J, Tysk C, Hettich RL, Jansson JK. 2009. Shotgun metaproteomics of the human distal gut microbiota. ISME J 3:179. https://doi.org/10.1038/ismej.2008.108.
34. Muthusamy S, Lundin D, Mamede Branca RM, Baltar F, González JM, Lehtiö J, Pinhassi J. 2017. Comparative proteomics reveals signature metabolisms of exponentially growing and stationary phase marine bacteria. Environ Microbiol 19:2301–2319. https://doi.org/10.1111/1462-2920.13725.
35. Steindler L, Schwalbach MS, Smith DP, Chan F, Giovannoni SJ. 2011. Energy starved *Candidatus* Pelagibacter ubique substitutes light-mediated ATP production for endogenous carbon respiration. PLoS One 6:e19725. https://doi.org/10.1371/journal.pone.0019725.
36. Giovannoni SJ, Bibbs L, Cho J-C, Stapels MD, Desiderio R, Vergin KL, Rappé MS, Laney S, Wilhelm LJ, Tripp HJ, Mathur EJ, Barofsky DF. 2005. Proteorhodopsin in the ubiquitous marine bacterium SAR11. Nature 438:82. https://doi.org/10.1038/nature04032.
37. Sowell SM, Wilhelm LJ, Norbeck AD, Lipton MS, Nicora CD, Barofsky DF, Carlson CA, Smith RD, Giovanonni SJ. 2009. Transport functions dominate the SAR11 metaproteome at low-nutrient extremes in the Sargasso Sea. ISME J 3:93. https://doi.org/10.1038/ismej.2008.83.
38. Cram JA, Parada AE, Fuhrman JA. 2016. Dilution reveals how viral lysis and grazing shape microbial communities. Limnol Oceanogr 61:889–905. https://doi.org/10.1002/lno.10259.
39. Ghylin TW, Garcia SL, Moya F, Oyserman BO, Schwientek P, Forest KT, Mutschler J, Dwulit-Smith J, Chan L-K, Martinez-Garcia M, Sczyrba A, Stepanauskas R, Grossart H-P, Woyke T, Warnecke F, Malmstrom R, Bertilsson S, McMahon KD. 2014. Comparative single-cell genomics reveals potential ecological niches for the freshwater acI *Actinobacteria* lineage. ISME J 8:2503. https://doi.org/10.1038/ismej.2014.135.
40. Kang I, Kim S, Islam MR, Cho J-C. 2017. The first complete genome sequences of the acI lineage, the most abundant freshwater *Actinobacteria*, obtained by whole-genome-amplification of dilution-to-extinction cultures. Sci Rep 7:42252. https://doi.org/10.1038/srep42252.
41. Warnecke F, Amann R, Pernthaler J. 2004. Actinobacterial 16S rRNA genes from freshwater habitats cluster in four distinct lineages. Environ Microbiol 6:242–253. https://doi.org/10.1111/j.1462-2920.2004.00561.x.
42. Farewell A, Diez AA, DiRusso CC, Nyström T. 1996. Role of the *Escherichia coli* FadR regulator in stasis survival and growth phase-dependent expression of the *uspA*, *fad*, and *fab* genes. J Bacteriol 178:6443–6450. https://doi.org/10.1128/jb.178.22.6443-6450.1996.
43. Hood MA, Guckert J, White D, Deck F. 1986. Effect of nutrient deprivation on lipid, carbohydrate, DNA, RNA, and protein levels in *Vibrio cholerae*. Appl Environ Microbiol 52:788–793.
44. Kaberdin VR, Montánchez I, Parada C, Orruño M, Arana I, Barcina I. 2015. Unveiling the metabolic pathways associated with the adaptive reduction of cell size during *Vibrio harveyi* persistence in seawater microcosms. Microb Ecol 70:689–700. https://doi.org/10.1007/s00248-015-0614-7.
45. Medema MH, Blin K, Cimermancic P, de Jager V, Zakrzewski P, Fischbach MA, Weber T, Takano E, Breitling R. 2011. antiSMASH: rapid identification, annotation and analysis of secondary metabolite biosynthesis gene clusters in bacterial and fungal genome sequences. Nucleic Acids Res 39:W339–W346. https://doi.org/10.1093/nar/gkr466.
46. Brunet YR, Khodr A, Logger L, Aussel L, Mignot T, Rimsky S, Cascales E. 2015. H-NS silencing of the *Salmonella* pathogenicity island 6-encoded type VI secretion system limits *Salmonella enterica* serovar Typhimurium interbacterial killing. Infect Immun 83:2738–2750. https://doi.org/10.1128/IAI.00198-15.
47. Payne JA, Schoppet M, Hansen MH, Cryle MJ. 2017. Diversity of nature's assembly lines–recent discoveries in non-ribosomal peptide synthesis. Mol Biosyst 13:9–22. https://doi.org/10.1039/C6MB00675B.
48. Süssmuth RD, Mainz A. 2017. Nonribosomal peptide synthesis-principles and prospects. Angew Chem Int Ed Engl 56:3770–3821. https://doi.org/10.1002/anie.201609079.
49. Arnison PG, Bibb MJ, Bierbaum G, Bowers AA, Bugni TS, Bulaj G, Camarero JA, Campopiano DJ, Challis GL, Clardy J, Cotter PD, Craik DJ, Dawson M, Dittmann E, Donadio S, Dorrestein PC, Entian K-D, Fischbach MA, Garavelli JS, Göransson U, Gruber CW, Haft DH, Hemscheidt TK, Hertweck C, Hill C, Horswill AR, Jaspars M, Kelly WL, Klinman JP, Kuipers OP, Link AJ, Liu W, Marahiel MA, Mitchell DA, Moll GN, Moore BS, Müller R, Nair SK, Nes IF, Norris GE, Olivera BM, Onaka H, Patchett ML, Piel J, Reaney MJT, Rebuffat S, Ross RP, Sahl H-G, Schmidt EW, Selsted ME, et al. 2013. Ribosomally synthesized and post-translationally modified peptide natural products: overview and recommendations for a universal nomenclature. Nat Prod Rep 30:108–160. https://doi.org/10.1039/c2np20085f.
50. Letzel AC, Li J, Amos GC, Millán-Aguiñaga N, Ginigini J, Abdelmohsen UR, Gaudêncio SP, Ziemert N, Moore BS, Jensen PR. 2017. Genomic insights into specialized metabolism in the marine actinomycete *Salinispora*. Environ Microbiol 19:3660–3673. https://doi.org/10.1111/1462-2920.13867.
51. Timmermans M, Paudel Y, Ross A. 2017. Investigating the biosynthesis of natural products from marine *Proteobacteria*: a survey of molecules and strategies. Mar Drugs 15:235. https://doi.org/10.3390/md15080235.
52. Gemperlein K, Zaburannyi N, Garcia R, La Clair J, Müller R. 2018. Metabolic and biosynthetic diversity in marine myxobacteria. Mar Drugs 16:314. https://doi.org/10.3390/md16090314.
53. Gasol JM, Zweifel UL, Peters F, Fuhrman JA, Hagström Å. 1999. Significance of size and nucleic acid content heterogeneity as measured by flow cytometry in natural planktonic bacteria. Appl Environ Microbiol 65:4475–4483.
54. Weinbauer MG, Fritz I, Wenderoth DF, Höfle MG. 2002. Simultaneous extraction from bacterioplankton of total RNA and DNA suitable for quantitative structure and function analyses. Appl Environ Microbiol 68:1082–1087. https://doi.org/10.1128/aem.68.3.1082-1087.2002.
55. Cole JR, Wang Q, Cardenas E, Fish J, Chai B, Farris RJ, Kulam-Syed-Mohideen AS, McGarrell DM, Marsh T, Garrity GM, Tiedje JM. 2009. The Ribosomal Database Project: improved alignments and new tools for rRNA analysis. Nucleic Acids Res 37:D141–D145. https://doi.org/10.1093/nar/gkn879.
56. Pruesse E, Quast C, Knittel K, Fuchs BM, Ludwig W, Peplies J, Glöckner FO. 2007. SILVA: a comprehensive online resource for quality checked and aligned ribosomal RNA sequence data compatible with ARB. Nucleic Acids Res 35:7188–7196. https://doi.org/10.1093/nar/gkm864.
57. Pruesse E, Peplies J, Glöckner FO. 2012. SINA: accurate high-throughput multiple sequence alignment of ribosomal RNA genes. Bioinformatics 28:1823–1829. https://doi.org/10.1093/bioinformatics/bts252.
58. Boisvert S, Raymond F, Godzaridis É, Laviolette F, Corbeil J. 2012. Ray Meta: scalable *de novo* metagenome assembly and profiling. Genome Biol 13:R122. https://doi.org/10.1186/gb-2012-13-12-r122.
59. Langmead B, Salzberg SL. 2012. Fast gapped-read alignment with Bowtie 2. Nat Methods 9:357. https://doi.org/10.1038/nmeth.1923.
60. Quinlan AR, Hall IM. 2010. BEDTools: a flexible suite of utilities for comparing genomic features. Bioinformatics 26:841–842. https://doi.org/10.1093/bioinformatics/btq033.
61. Markowitz VM, Chen I-MA, Palaniappan K, Chu K, Szeto E, Grechkin Y, Ratner A, Jacob B, Huang J, Williams P, Huntemann M, Anderson I,

Mavromatis K, Ivanova NN, Kyrpides NC. 2012. IMG: the integrated microbial genomes database and comparative analysis system. Nucleic Acids Res 40:D115–D122. https://doi.org/10.1093/nar/gkr1044.
62. Camacho C, Coulouris G, Avagyan V, Ma N, Papadopoulos J, Bealer K, Madden TL. 2009. BLAST+: architecture and applications. BMC Bioinformatics 10:421. https://doi.org/10.1186/1471-2105-10-421.
63. Saier MH, Jr, Tran CV, Barabote RD. 2006. TCDB: the Transporter Classification Database for membrane transport protein analyses and information. Nucleic Acids Res 34:D181–D186. https://doi.org/10.1093/nar/gkj001.
64. Marchler-Bauer A, Lu S, Anderson JB, Chitsaz F, Derbyshire MK, DeWeese-Scott C, Fong JH, Geer LY, Geer RC, Gonzales NR, Gwadz M, Hurwitz DI, Jackson JD, Ke Z, Lanczycki CJ, Lu F, Marchler GH, Mullokandov M, Omelchenko MV, Robertson CL, Song JS, Thanki N, Yamashita RA, Zhang D, Zhang N, Zheng C, Bryant SH. 2011. CDD: a Conserved Domain Database for the functional annotation of proteins. Nucleic Acids Res 39:D225–D229. https://doi.org/10.1093/nar/gkq1189.
65. Fu L, Niu B, Zhu Z, Wu S, Li W. 2012. CD-HIT: accelerated for clustering the next-generation sequencing data. Bioinformatics 28:3150–3152. https://doi.org/10.1093/bioinformatics/bts565.
66. Eymann C, Dreisbach A, Albrecht D, Bernhardt J, Becher D, Gentner S, Tam LT, Büttner K, Buurman G, Scharf C, Venz S, Völker U, Hecker M. 2004. A comprehensive proteome map of growing *Bacillus subtilis* cells. Proteomics 4:2849–2876. https://doi.org/10.1002/pmic.200400907.
67. Ponnudurai R, Kleiner M, Sayavedra L, Petersen JM, Moche M, Otto A, Becher D, Takeuchi T, Satoh N, Dubilier N, Schweder T, Markert S. 2017. Metabolic and physiological interdependencies in the *Bathymodiolus azoricus* symbiosis. ISME J 11:463. https://doi.org/10.1038/ismej.2016.124.
68. Heinz E, Williams TA, Nakjang S, Noël CJ, Swan DC, Goldberg AV, Harris SR, Weinmaier T, Markert S, Becher D, Bernhardt J, Dagan T, Hacker C, Lucocq JM, Schweder T, Rattei T, Hall N, Hirt RP, Embley TM. 2012. The genome of the obligate intracellular parasite *Trachipleistophora hominis*: new insights into microsporidian genome dynamics and reductive evolution. PLoS Pathog 8:e1002979. https://doi.org/10.1371/journal.ppat.1002979.
69. Florens L, Carozza MJ, Swanson SK, Fournier M, Coleman MK, Workman JL, Washburn MP. 2006. Analyzing chromatin remodeling complexes using shotgun proteomics and normalized spectral abundance factors. Methods 40:303–311. https://doi.org/10.1016/j.ymeth.2006.07.028.
70. Vizcaíno JA, Csordas A, del-Toro N, Dianes JA, Griss J, Lavidas I, Mayer G, Perez-Riverol Y, Reisinger F, Ternent T, Xu Q-W, Wang R, Hermjakob H. 2016. 2016 update of the PRIDE database and its related tools. Nucleic Acids Res 44:D447–D456. https://doi.org/10.1093/nar/gkv1145.